https://doi.org/10.15407/ujpe69.9.671

I.R. YUKHNOVSKII, R.V. ROMANIK

Institute for Condensed Matter Physics, Nat. Acad. of Sci. of Ukraine
(1, Svientsitskii Str., Lviv 79011, Ukraine; e-mail: romanik@icmp.lviv.ua)

CRITICAL TEMPERATURE DETERMINATION FOR SIMPLE FLUIDS: AN ANALYTICAL APPROACH BASED ON COLLECTIVE VARIABLES METHOD

An explicit equation for the liquid-vapor critical temperature of simple fluids is derived within an analytic approach – the method of collective variables with a reference system. This equation is applied to calculate the critical temperature values for several hard-core van der Waals fluids. The study also examines how the critical temperature depends on parameters of the interaction. Specifically, it is observed that, as the range of attractive interaction decreases, the critical temperature decreases as well.

K e y w o r d s: simple fluids, collective variables, critical temperature.

1. Introduction

Nowadays, computer simulations seem to be the most common tool to study the equilibrium properties of simple fluids. Still, analytic theories that enable the calculation of thermodynamic properties for many-particle interacting systems remain invaluable, as they may provide physical understanding that might otherwise be missed. One such theory is built around the collective variables (CV) method [1] with a reference system (RS) [2]. A general overview of this approach and the results obtained in its framework for liquid systems near the liquid-vapor critical point can be found in [3]. For an overview of the general state of the physics of fluids, we refer to [4, 5]. In this paper, we focus on the details of determining the critical temperature and how the parameters of the attractive interaction affect this temperature.

The structure of this paper is as follows. In Section 2, we present a functional of the grand partition function (GPF), with all coefficients explicitly defined. Then we proceed with the "layer-by-layer" integration of that functional to obtain a sequence of effective block Hamiltonians, each characterized by its own coefficients. After the result of the integration over n layers is written down in a generic form, we pass to the analysis of the recurrence relations between the effective Hamiltonian coefficients. As a result, we find the fixed point solution, write the recurrence relations in the linear approximation around the fixed point, and find a condition that leads to the equation for the critical temperature. In Section 3, we briefly discuss the interaction potentials and applied approximations. In Section 4, we calculate the critical temperature for different hard-core (HC) van der Waals fluids using the derived expression and compare the obtained values with known results for the considered models.

2. Grand Partition Function in the Representation of Collective Variables

The GPF of a simple many-particle interacting system can be represented as [2, 6, 7]

$$\Xi = \Xi_0 \, \Xi_G \, \Xi_L. \tag{1}$$

Here Ξ_0 is the GPF of a RS, which is assumed to be known. Ξ_G is a short-wave contribution to the GPF with wave-vectors $|\mathbf{k}| > B_0$, B_0 being the cut-off parameter. The quantity Ξ_L denotes long-wave contributions to the GPF and is the object of our investigation in this paper. In our previous paper [7] we provided very detailed derivation of the expression for Ξ_L (see [8] for even more details) and presented

C i t a t i o n: Yukhnovskii I.R., Romanik R.V. Critical temperature determination for simple fluids: an analytical approach based on collective variables method. *Ukr. J. Phys.* **69**, No. 9, 671 (2024). https://doi.org/10.15407/ujpe69.9.671.

it as follows:

$$\Xi_L = j_0 Q(\tilde{\mathfrak{M}}_2, \mathfrak{M}_4)^{N_0} \exp(\tilde{\mathfrak{M}}_0)\Xi_L^{(1)}, \tag{2}$$

where $j_0 = \sqrt{2}^{N_0-1}$, N_0 being determined in (4) below, $Q(\tilde{\mathfrak{M}}_2, \mathfrak{M}_4)$ and $\tilde{\mathfrak{M}}_0$ are explicitly given in Appendix A.

The quantity $\Xi_L^{(1)}$ in the approximation of the so-called ρ^4 model is given by

$$\Xi_L^{(1)} = \int \exp\Bigg(\mu^*\rho_0 - \frac{1}{2}\sum_{\substack{\mathbf{k}\\ k\le B_0}} d_2(k)\rho_{\mathbf{k}}\rho_{-\mathbf{k}} - \\ - \frac{a_4}{4!N_0}\sum_{\substack{\mathbf{k}_1,\ldots,\mathbf{k}_4\\ k_i\le B_0}} \rho_{\mathbf{k}_1}\ldots\rho_{\mathbf{k}_4}\delta_{\mathbf{k}_1+\ldots+\mathbf{k}_4}\Bigg)(\mathrm{d}\rho)^{N_0}. \tag{3}$$

Here, $d_2(k) = a_2 + \frac{\beta\hat{\Phi}_{\mathbf{k}}}{V}$, β being the inverse temperature, V the volume, $\hat{\Phi}_{\mathbf{k}}$ the Fourier component of the long-range part of the interaction potential. Quantities μ^*, a_2 and a_4 are functions of the RS particle density ρ, temperature T, and microscopic parameters of the interaction potential. They are explicitly presented in Appendix A. The quantity μ^* also linearly depends on the chemical potential μ.

The wave vector $\mathbf{k}$ takes on N_0 values in a sphere of radius B_0, so that

$$N_0 = \frac{B_0^3}{6\pi^2}V. \tag{4}$$

Thus, the number of variables to be integrated over is equal to N_0

$$(d\rho)^{N_0} = \mathrm{d}\rho_0 \prod_{\substack{\mathbf{k}\\ k\le B_0}}{}' \mathrm{d}\rho_{\mathbf{k}}^c \mathrm{d}\omega_{\mathbf{k}}^s$$

where $\rho_{\mathbf{k}}^c$ and $\rho_{\mathbf{k}}^s$ are the real and imaginary parts of the CV $\rho_{\mathbf{k}} = \rho_{\mathbf{k}}^c - \mathrm{i}\rho_{\mathbf{k}}^s$, respectively [1]. The 'prime' sign over the product means that the wave-vector takes on values only form the upper semi-sphere, i.e., $k_z > 0$ and $|\mathbf{k}| \neq 0$.

[1] Traditionally, the collective variables are denoted by $\rho_{\mathbf{k}}$, and the element of integration over CVs is denoted by $(\mathrm{d}\rho)$, while the particle density is denoted by ρ. We hope that it is clear from the context when ρ is understood as the number density, and when it is related to CVs.

The following simplification is used for the Kronecker symbol in (3)

$$\delta_{\mathbf{k}} = \frac{1}{V}\int \mathrm{e}^{-\mathrm{i}\mathbf{k}\mathbf{r}}\,\mathrm{d}\mathbf{r} = \frac{1}{N_0}\sum_{\mathbf{l_0}} \mathrm{e}^{-\mathrm{i}\mathbf{k}\mathbf{l}_0}.$$

The summation over $\mathbf{l}_0$ implies that $\mathbf{l}_0$ takes on N_0 values in real space corresponding to the N_0 values of the wave vector $\mathbf{k}$ in a sphere of radius B_0 in the reciprocal space. This is called a spherical approximation for the first Brillouin zone. It is assumed that a proper correspondence can be established between a spherical Brillouin zone and a structure in real space by analogy to how simple cubic lattice corresponds to its Brillouin zone in the Ising-model problem [9].

In what follows, we also will understand that $\mathbf{l} \in \Lambda_0$ corresponds to vectors $\mathbf{k}$ such that $k \le B_0$, $\mathbf{l} \in \Lambda_1$ to $k \le B_1$, and, in general, $\mathbf{l} \in \Lambda_n$ to $k \le B_n$. Here, $B_n = B_0/s^n$, and s is the renormalization parameter to be introduced later.

The expression (3) formally coincides with the expression for the partition function functional of the 3-dimentional Ising-like model in an external field [10, 11]. It is not surprising with regard for that both the simple fluids and the Ising model belong to the same class of universality. One can go even further and consider the idea of a global isomorphism and its applications [12, 13].

A necessary condition for the functional (3) to give rise to a critical-point solution is $\mu^* = 0$, which leads to a line of critical temperature dependence on the chemical potential μ (at some value of the RS particle density ρ_c) [7].

We are going to integrate (3) following the method developed for calculation of the partition function of the 3-dimentional Ising-like models [9, 14, 15]. The main idea is to divide the interval $[0, B_0]$ into subintervals $(B_1, B_0]$, $(B_2, B_1]$, $(B_3, B_2]$ and so on, where $B_1 = B_0/s$, $B_2 = B_1/s = B_2/s^2$, or, in general, $B_n = B_0/s^n$, s being the renormalization group parameter, $s > 1$. Variables $\rho_{\mathbf{k}}$ with $B_1 < k \le B_0$ are said to belong to the first layer, $\rho_{\mathbf{k}}$ with $B_2 < k \le B_1$ to the second one, and, continuing in the same manner, $\rho_{\mathbf{k}}$ with $B_n < k \le B_{n-1}$ to the n-th layer. The integration is performed iteratively, starting with integration over the CVs of the first layer, then over the second one and so on. The number of variables to be left after the integration over the first layer is $N_1 = N_0/s^3 = (B_0^3 V)/(2\pi^2 s^3)$. Thus, the num-

ber of variables integrated out in the first iteration is $N_0 - N_1 = N_0(1 - s^{-3})$.

To factorize the integrals, the Fourier transform $\hat{\Phi}_{\mathbf{k}}$ of the long-range part of interaction potential is replaced with its average value over each interval:

$$\begin{aligned}\hat{\Phi}_{\mathbf{k}} \;\to\; & \hat{\Phi}_{B_1,B_0}, \quad B_1 < k \le B_0;\\ & \hat{\Phi}_{B_2,B_1}, \quad B_2 < k \le B_1;\\ & \cdots\\ & \hat{\Phi}_{B_n,B_{n-1}}, \quad B_n < k \le B_{n-1}.\end{aligned}$$

The particulars of this averaging are not so important to outline the method of layer-by-layer integration. Thus, we will return to them later, when we present some numerical and graphical results. Note that we postpone the specifying of the interaction potential details to a later stage of the paper. For now, we just restrict it to a form that it can be (quite freerely) separated into short-range repulsive and long-range attractive counterparts. The properties of the short-range one are assumed to be known. One of the required properties for the long-range part is that it possesses a Fourier transform, and the long-wave limit ($|\mathbf{k}| = 0$) of it takes on a negative value.

2.1. Integration over the first layer

Now, let us explicitly integrate over the variables of the first layer. During the course of integration, we closely follow steps described in [15].

The second term in the exponent of (3) is rewritten as

$$\sum_{\mathbf{k},\, k\le B_0} d_2(k)\rho_{\mathbf{k}}\rho_{-\mathbf{k}} = \sum_{\mathbf{k},\, k\le B_1} d_2(k)\rho_{\mathbf{k}}\rho_{-\mathbf{k}} + \\ + \sum_{\mathbf{k},\, B_1<k\le B_0} d_2(B_1,B_0)\rho_{\mathbf{k}}\rho_{-\mathbf{k}},$$

where $d_2(B_1,B_0) = a_2 + \beta\hat{\Phi}_{B_1,B_0}/V$. The expression for $\Xi_L^{(1)}$ is now recast

$$\Xi_L^{(1)} = \int \exp\Bigg(\mu^*\rho_0 - \frac{1}{2}\sum_{\substack{\mathbf{k}\\ k\le B_1}} d_2(k)\rho_{\mathbf{k}}\rho_{-\mathbf{k}} - \\ - \frac{d_2(B_1,B_0)}{2}\sum_{\substack{\mathbf{k}\\ B_1<k\le B_0}} \rho_{\mathbf{k}}\rho_{-\mathbf{k}} - \\ - \frac{a_4}{4!N_0}\sum_{\substack{\mathbf{k_1},\ldots,\mathbf{k}_4\\ k_i\le B_0}} \rho_{\mathbf{k}_1}\cdots\rho_{\mathbf{k}_4}\delta_{\mathbf{k}_1+\ldots+\mathbf{k}_4}\Bigg)\times \\ \times (\mathrm{d}\rho)^{N_1}(\mathrm{d}\rho)^{N_0-N_1}.$$

To distinguish the variables to be integrated over in the first iteration, let us denote them by $\eta_{\mathbf{k}}$, i.e., $\rho_{\mathbf{k}} \to \\ \to \eta_{\mathbf{k}}$ for $B_1 < k \le B_0$. Let us also extend the number of variables $\eta_{\mathbf{k}}$ with the help of $\delta-$functions:

$$\prod_{\mathbf{k},\, 0\le k\le B_1} \delta(\eta_{\mathbf{k}} - \rho_{\mathbf{k}}) = \int (\mathrm{d}\nu)^{N_1}\times \\ \times \exp(2\pi\mathrm{i}\sum_{k\le B_1}\nu_{\mathbf{k}}(\eta_{\mathbf{k}} - \rho_{\mathbf{k}}))$$

so that $\Xi_L^{(1)}$ is rewritten as

$$\Xi_L^{(1)} = \int (\mathrm{d}\rho)^{N_1}\exp\Bigg(\mu^*\rho_0 - \\ - \frac{1}{2}\sum_{\substack{\mathbf{k}\\ k\le B_1}} (d_2(k) - d_2(B_1,B_0))\rho_{\mathbf{k}}\rho_{-\mathbf{k}}\Bigg)\times \\ \times \int (\mathrm{d}\nu)^{N_1}\exp\Bigg(-2\pi\mathrm{i}\sum_{\mathbf{k},\,\mathbf{k}\le\mathbf{B_1}}\nu_{\mathbf{k}}\rho_{\mathbf{k}}\Bigg) I(\nu_{\mathbf{k}}).$$

Here the notation $I(\nu_{\mathbf{k}})$ stands for the integral over $\eta_{\mathbf{k}}$

$$I(\nu_{\mathbf{k}}) = \int (\mathrm{d}\eta)^{N_0}\exp\Bigg(2\pi\mathrm{i}\sum_{\mathbf{k},\, k\le B_0}\bar{\nu}_{\mathbf{k}}\eta_{\mathbf{k}} - \\ - \frac{d_2(B_1,B_0)}{2}\sum_{\mathbf{k},\, k\le B_0}\eta_{\mathbf{k}}\eta_{-\mathbf{k}} - \\ - \frac{a_4}{4!N_0}\sum_{\substack{\mathbf{k}_1,\ldots,\mathbf{k}_4\\ k_i\le B_0}}\eta_{\mathbf{k}_1}\cdots\eta_{\mathbf{k}_4}\delta_{\mathbf{k}_1+\ldots+\mathbf{k}_4}\Bigg),$$

where the quantity $\bar{\nu}_{\mathbf{k}}$ is introduced as

$$\bar{\nu}_{\mathbf{k}} = \begin{cases}\nu_{\mathbf{k}}, & k \le B_1,\\ 0, & B_1 < k \le B_0\end{cases}$$

by analogy with the method described in [15].

Now, this integral can be factorized in the so-called site variables

$$\tilde{\eta}_{\mathbf{l}} = \frac{1}{\sqrt{N_0}}\sum_{\mathbf{k},\, k\le B_0}\eta_{\mathbf{k}}\mathrm{e}^{\mathrm{i}\mathbf{k}\mathbf{l}},$$

$$\tilde{\bar{\nu}}_{\mathbf{l}} = \frac{1}{\sqrt{N_0}}\sum_{\mathbf{k},\, k\le B_0}\bar{\nu}_{\mathbf{k}}\mathrm{e}^{-\mathrm{i}\mathbf{k}\mathbf{l}}.$$

For some useful relations for site variables, see Appendix B. Now, the integral takes on the form

$$I(\nu_{\mathbf{k}}) = j_0^{-1}\prod_{\mathbf{l}\in\Lambda_0}\int_{-\infty}^{\infty}\mathrm{d}\tilde{\eta}_{\mathbf{l}}\exp\Bigg(2\pi\mathrm{i}\tilde{\bar{\nu}}_{\mathbf{l}}\tilde{\eta}_{\mathbf{l}} -$$

$$-\frac{d_2(B_1,B_0)}{2}\tilde{\eta}_{\mathbf{l}}{}^2-\frac{a_4}{4!}\tilde{\eta}_{\mathbf{l}}{}^4\Bigg)=$$
$$=j_0^{-1}[Q_{f_0}]^{N_0}\prod_{\mathbf{l}\in\mathbf{\Lambda_0}}\exp\left(-\sum_{n\geq 1}\frac{S_{2n}}{(2n)!}\tilde{\nu}_{\mathbf{l}}^{2n}\right).$$

Restricting the resulting exponent to the 4-th power in $\tilde{\nu}_{\mathbf{l}}$, we get

$$I(\nu_{\mathbf{k}})=j_0^{-1}[Q_{f_0}]^{N_0}\prod_{\mathbf{l}\in\Lambda_0}\exp\left(-\frac{S_2}{2!}\tilde{\nu}_{\mathbf{l}}^2-\frac{S_4}{4!}\tilde{\nu}_{\mathbf{l}}^4\right).$$

In terms of $\nu_{\mathbf{k}}$ the result for $I(\nu_{\mathbf{k}})$ is expressed as follows:

$$I(\nu_{\mathbf{k}})=j_0^{-1}[Q_{f_0}]^{N_0}\exp\Bigg(-\frac{S_2}{2!}\sum_{\mathbf{k},k\leq B_1}\nu_{\mathbf{k}}\nu_{-\mathbf{k}}$$
$$-\frac{S_4}{4!N_0}\sum_{\substack{\mathbf{k_1},\ldots,\mathbf{k_4}\\ k_i\leq B_1}}\nu_{\mathbf{k_1}}\ldots\nu_{\mathbf{k_4}}\delta_{\mathbf{k}_1+\ldots+\mathbf{k}_4}\Bigg).$$

In the above formulae, the following quantities were introduced:

$$Q_{f_0}=\sqrt{2\pi}\left(\frac{3}{a_4}\right)^{1/4}\mathrm{e}^{x^2/4}U(0,x);$$
$$S_2=(2\pi)^2\left(\frac{3}{a_4}\right)^{1/2}U(x);\quad S_4=(2\pi)^4\frac{3}{a_4}\varphi(x);$$
$$x=d_2(B_1,B_0)\left(\frac{3}{a_4}\right)^{1/2}.$$

The next step is to integrate, over $\nu_{\mathbf{k}}$, the following integral

$$I_2(\rho_{\mathbf{k}})=\int(\mathrm{d}\nu)^{N_1}\exp\Bigg(-2\pi\mathrm{i}\sum_{\mathbf{k},\,k\leq B_1}\nu_{\mathbf{k}}\rho_{\mathbf{k}}-$$
$$-\frac{S_2}{2!}\sum_{\mathbf{k},\,k\leq B_1}\nu_{\mathbf{k}}\nu_{-\mathbf{k}}-$$
$$-\frac{S_4 s^{-3}}{4!N_1}\sum_{\substack{\mathbf{k}_1,\ldots,\,\mathbf{k}_4\\ k_i\leq B_1}}\nu_{\mathbf{k}_1}\ldots\nu_{\mathbf{k}_4}\delta_{\mathbf{k}_1+\ldots+\mathbf{k}_4}\Bigg)=$$
$$=j_1\prod_{\mathbf{l}\in\Lambda_1}\int\mathrm{d}\tilde{\nu}_{\mathbf{l}}\exp(-2\pi\mathrm{i}\tilde{\nu}_{\mathbf{l}}\tilde{\rho}_{\mathbf{l}})\times$$
$$\times\exp\left(-\frac{S_2}{2!}\tilde{\nu}_{\mathbf{l}}^2-\frac{S_4}{4!s^3}\tilde{\nu}_{\mathbf{l}}^4\right),$$

where $j_1=\sqrt{2}^{N_1-1}$, and this time

$$\tilde{\rho}_{\mathbf{l}}=\frac{1}{\sqrt{N_1}}\sum_{\mathbf{k},k\leq B_1}\rho_{\mathbf{k}}\mathrm{e}^{\mathrm{i}\mathbf{kl}},$$
$$\tilde{\nu}_{\mathbf{l}}=\frac{1}{\sqrt{N_1}}\sum_{\mathbf{k},k\leq B_1}\nu_{\mathbf{k}}\mathrm{e}^{-\mathrm{i}\mathbf{kl}}.$$

The result of the integration is

$$I_2(\rho_{\mathbf{k}})=j_1[Q_{\varphi_0}]^{N_1}\prod_{\mathbf{l}\in\Lambda_1}\exp\left(-\sum_{n\geq 1}\frac{R_{2n}}{(2n)!}\tilde{\rho}_{\mathbf{l}}^{2n}\right).$$

In the "ρ^4" approximation, this takes the form

$$I_2(\rho_{\mathbf{k}})=j_1[Q_{\varphi_0}]^{N_1}\prod_{\mathbf{l}\in\Lambda_1}\exp\left(-\frac{R_2}{2!}\tilde{\rho}_{\mathbf{l}}^2-\frac{R_4}{4!}\tilde{\rho}_{\mathbf{l}}^4\right)=$$
$$=j_1[Q_{\varphi_0}]^{N_1}\exp\Bigg(-\frac{R_2}{2!}\sum_{\mathbf{k},k\leq B_1}\rho_{\mathbf{k}}\rho_{-\mathbf{k}}-$$
$$-\frac{R_4}{4!N_1}\sum_{\substack{\mathbf{k}_1,\ldots,\,\mathbf{k}_4\\ k_i\leq B_1}}\rho_{\mathbf{k}_1}\ldots\rho_{\mathbf{k}_4}\delta_{\mathbf{k}_1+\ldots+\mathbf{k}_4}\Bigg).$$

Here,

$$Q_{\varphi_0}=(2\pi)^{-1/2}s^{3/4}\left(\frac{a_4}{\varphi(x)}\right)^{1/4}\mathrm{e}^{y^2/4}U(0,y);$$
$$R_2=s^{3/2}\left(\frac{a_4}{\varphi(x)}\right)^{1/2}U(y);\quad R_4=s^3a_4\frac{\varphi(y)}{\varphi(x)};$$
$$y=s^{3/2}U(x)\sqrt{\frac{3}{\varphi(x)}}.$$

This time, the approximation for the Kronecker symbol is

$$\delta_{\mathbf{k}}\approx\frac{1}{N_1}\sum_{\mathbf{l}\in\mathbf{\Lambda_1}}\exp(-\mathrm{i}\mathbf{kl}).$$

Finally, as a result of the integration over the first layer, we get, for $\Xi_L^{(1)}$,

$$\Xi_L^{(1)}=j_0^{-1}j_1[Q_{f_0}]^{N_0}[Q_{\varphi_0}]^{N_1}\times$$
$$\times\int(\mathrm{d}\rho)^{N_1}\exp\Bigg(\mu^*\rho_0-\frac{1}{2}\sum_{\mathbf{k},\,k\leq B_1}d_2^{(1)}(k)\rho_{\mathbf{k}}\rho_{-\mathbf{k}}-$$
$$-\frac{a_4^{(1)}}{4!N_1}\sum_{\substack{\mathbf{k}_1,\ldots,\,\mathbf{k}_4\\ k_i\leq B_1}}\rho_{\mathbf{k}_1}\ldots\rho_{\mathbf{k}_4}\delta_{\mathbf{k}_1+\ldots+\mathbf{k}_4}\Bigg),$$

where

$$d_2^{(1)}(k)=a_2^{(1)}+\beta\hat{\Phi}_{\mathbf{k}}/V;\qquad(5)$$
$$a_2^{(1)}=R_2-\frac{\beta\hat{\Phi}_{B_1,B_0}}{V}=$$
$$=s^{3/2}\left(\frac{a_4}{\varphi(x)}\right)^{1/2}U(y)-\frac{\beta\hat{\Phi}_{B_1,B_0}}{V};\qquad(6)$$

$$a_4^{(1)} = R_4 = s^3 a_4 \frac{\varphi(y)}{\varphi(x)}. \quad (7)$$

These are recurrence relations between coefficients of an effective Hamiltonian before and after the integration over the first layer, establishing expressions for coefficients $a_2^{(1)}$ and $a_4^{(1)}$ via a_2 and a_4. An alternative, the concise form is

$$a_2^{(1)} = d_2(B_1, B_0)N(x) - \frac{\beta\hat{\Phi}_{B_1,B_0}}{V}; \quad (8)$$

$$a_4^{(1)} = s^{-3} a_4 E(x). \quad (9)$$

Here, the following quantities are introduced

$$N(x) = \frac{yU(y)}{xU(x)}; \quad E(x) = s^6 \frac{\varphi(y)}{\varphi(x)}.$$

2.2. Integration over the second layer

Following the outlined procedure, we can perform the integration over the second layer with $B_2 < k \leq \leq B_1$. As a result of such integration, the quantity $\Xi_L^{(1)}$ takes on the following expression:

$$\Xi_L^{(1)} = j_0^{-1} j_2 [Q_{f_0}]^{N_0} [Q_{\varphi_0}]^{N_1} [Q_{f_1}]^{N_1} [Q_{\varphi_1}]^{N_2} \times$$

$$\times \int (\mathrm{d}\rho)^{N_2} \exp\left(\mu^* \rho_0 - \frac{1}{2} \sum_{\mathbf{k},\, k \leq B_2} d_2^{(2)}(k) \rho_{\mathbf{k}} \rho_{-\mathbf{k}} - \right.$$

$$\left. - \frac{a_4^{(2)}}{4! N_2} \sum_{\substack{\mathbf{k}_1,\ldots,\mathbf{k}_4 \\ k_i \leq B_2}} \rho_{\mathbf{k}_1} \ldots \rho_{\mathbf{k}_4} \delta_{\mathbf{k}_1 + \ldots + \mathbf{k}_4} \right),$$

where $j_2 = \sqrt{2}^{N_2 - 1}$, and

$$d_2^{(2)}(k) = a_2^{(2)} + \beta\hat{\Phi}_{\mathbf{k}}/V; \quad (10)$$

$$a_2^{(2)} = R_2^{(1)} - \frac{\beta\hat{\Phi}_{B_2,B_1}}{V} =$$

$$= s^{3/2} \left(\frac{a_4^{(1)}}{\varphi(x_1)}\right)^{1/2} U(y_1) - \frac{\beta\hat{\Phi}_{B_2,B_1}}{V}; \quad (11)$$

$$a_4^{(2)} = R_4^{(1)} = s^3 a_4^{(1)} \frac{\varphi(y_1)}{\varphi(x_1)}. \quad (12)$$

The other quantities are

$$R_2^{(1)} = s^{3/2} \left(\frac{a_4^{(1)}}{\varphi(x_1)}\right)^{1/2} U(y_1);$$

$$R_4^{(1)} = s^3 a_4^{(1)} \frac{\varphi(y_1)}{\varphi(x_1)};$$

$$y_1 = s^{3/2} U(x_1) \left(\frac{3}{\varphi(x_1)}\right)^{1/2};$$

$$x_1 = d_2^{(1)}(B_2, B_1) \left(\frac{3}{a_4^{(1)}}\right)^{1/2}.$$

$$Q_{f_1} = \sqrt{2\pi} \left(\frac{3}{a_4^{(1)}}\right)^{1/4} \mathrm{e}^{x_1^2/4} U(0, x_1);$$

$$Q_{\varphi_1} = (2\pi)^{-1/2} s^{3/4} \left(\frac{a_4^{(1)}}{\varphi(x_1)}\right)^{1/4} \mathrm{e}^{y_1^2/4} U(0, y_1).$$

The recurrence relations (10)–(12) link the coefficients of an effective Hamiltonian before and after the integration over the second layer, expressing coefficients $a_2^{(2)}$ and $a_4^{(2)}$ via $a_2^{(1)}$ and $a_4^{(1)}$. They are analogous to Eqs. (5)–(7). Written in a concise form analogous to Eqs. (8) and (9), they are

$$a_2^{(2)} = d_2^{(1)}(B_2, B_1)N(x_1) - \frac{\beta\hat{\Phi}_{B_2,B_1}}{V}; \quad (13)$$

$$a_4^{(2)} = s^{-3} a_4^{(1)} E(x_1). \quad (14)$$

2.3. General result for the layer-by-layer integration

Having noticed the pattern at the integration over the first two layers, we are now ready to generalize the result for an arbitrary number of layers.

$$\Xi_L^{(1)} = j_0^{-1} j_n Q_0 Q_1 \ldots Q_{n-1} \times$$

$$\times \int (\mathrm{d}\rho)^{N_n} \exp\left(\mu^* \rho_0 - \frac{1}{2} \sum_{\mathbf{k}, k \leq B_n} d_2^{(n)}(k) \rho_{\mathbf{k}} \rho_{-\mathbf{k}} = \right.$$

$$\left. = \frac{a_4^{(n)}}{4! N_n} \sum_{\substack{\mathbf{k}_1,\ldots,\mathbf{k}_4 \\ k_i \leq B_n}} \rho_{\mathbf{k}_1} \ldots \rho_{\mathbf{k}_4} \delta_{\mathbf{k}_1 + \ldots + \mathbf{k}_4} \right),$$

where $j_n = \sqrt{2}^{N_n - 1}$, and

$$d_2^{(n)}(k) = a_2^{(n)} + \beta\hat{\Phi}_{\mathbf{k}}/V; \quad (15)$$

$$a_2^{(n)} = R_2^{(n-1)} - \frac{\beta\hat{\Phi}_{B_n,B_{n-1}}}{V} =$$

$$= s^{3/2} \left(\frac{a_4^{(n-1)}}{\varphi(x_{n-1})}\right)^{1/2} U(y_{n-1}) - \frac{\beta\hat{\Phi}_{B_n,B_{n-1}}}{V}; \quad (16)$$

$$a_4^{(n)} = R_4^{(n-1)} = s^3 a_4^{(n-1)} \frac{\varphi(y_{n-1})}{\varphi(x_{n-1})}. \quad (17)$$

The other quantities are

$$R_2^{(n)} = s^{3/2}\left(\frac{a_4^{(n)}}{\varphi(x_n)}\right)^{1/2} U(y_n);$$

$$R_4^{(n)} = s^3 a_4^{(n)} \frac{\varphi(y_n)}{\varphi(x_n)},$$

$$y_n = s^{3/2} U(x_n)\left(\frac{3}{\varphi(x_n)}\right)^{1/2},$$

$$x_n = d_2^{(n)}(B_{n+1}, B_n)\left(\frac{3}{a_4^{(n)}}\right)^{1/2}.$$

$$Q_n = Q_{f_n}^{N_n} Q_{\varphi_n}^{N_{n+1}};$$

$$Q_{f_n} = \sqrt{2\pi}\left(\frac{3}{a_4^{(n)}}\right)^{1/4} \mathrm{e}^{x_n^2/4} U(0, x_n);$$

$$Q_{\varphi_n} = (2\pi)^{-1/2} s^{3/4}\left(\frac{a_4^{(n)}}{\varphi(x_n)}\right)^{1/4} \mathrm{e}^{y_n^2/4} U(0, y_n).$$

A concise form of the recurrence relations is as follows:

$$a_2^{(n)} = d_2^{(n-1)}(B_n, B_{n-1}) N(x_{n-1}) - \frac{\beta\hat{\Phi}_{B_n, B_{n-1}}}{V};$$
$$a_4^{(n)} = s^{-3} a_4^{(n-1)} E(x_{n-1}).$$

2.4. Recurrence relations

The general recurrence relations between coefficients of effective block-structure Hamiltonians can be written in the form

$$a_2^{(n+1)} = d_2^{(n)}(B_{n+1}, B_n) N(x_n) - \frac{\beta\hat{\Phi}_{B_{n+1}, B_n}}{V}; \quad (18)$$
$$a_4^{(n+1)} = s^{-3} a_4^{(n)} E(x_n). \quad (19)$$

With the help of the following change of variables

$$r_n = d_2^{(n)}(0) s^{2n},$$
$$u_n = a_4^{(n)} s^{4n}$$

the recurrence relations become

$$r_{n+1} = s^2(r_n + q) N(x_n) - s^2 q;$$
$$u_{n+1} = s u_n E(x_n). \quad (20)$$

Here

$$q = s^{2n}\frac{\beta\hat{\Phi}_0}{V}\left(\frac{\hat{\Phi}_{B_{n+1}, B_n}}{\hat{\Phi}_0} - 1\right) = -\frac{\beta\hat{\Phi}_0}{V}\bar{q},$$

where

$$\bar{q} = -s^{2n}\left(\frac{\hat{\Phi}_{B_{n+1}, B_n}}{\hat{\Phi}_0} - 1\right).$$

The recurrence relations (20) possess a fixed point solution in the limit of $n \to \infty$. By definition, the fixed point solution means

$$r_{n+1} = r_n = r^*; \quad u_{n+1} = u_n = u^*$$

and hence

$$r^* = s^2[-q + (r^* + q) N(x^*)],$$
$$u^* = s u^* E(x^*).$$

From the last equality, it follows

$$sE(x^*) = 1.$$

It is practical to chose $x^* = 0$, which is equivalent to $\lim_{n\to\infty} d_2^{(n)}(0) = d_2^* = 0$ at the fixed point and gives $s = s^* = 3.5862$. We will use this value of s to obtain particular numerical and graphical results. From the first recurrence relation, it follows

$$r^* = -q\frac{N(x^*) - 1}{N(x^*) - s^{-2}}.$$

At $x^* = 0$, $r^* = -q$, because

$$\lim_{x\to 0}\frac{N(x) - 1}{N(x) - s^{-2}} = 1.$$

Finally, from

$$x^* = \sqrt{3}\frac{r^* + q}{\sqrt{u^*}}$$

we find the following expression for u^*

$$u^* = \frac{3q^2}{(x^*)^2}\left[\frac{1 - s^{-2}}{N(x^*) - s^{-2}}\right]^2.$$

We can write down the coordinates of the fixed point (for details on $\hat{\Phi}_0$, see Subsection 3):

$$r^* = -\frac{\beta|\hat{\Phi}_0|}{V}\bar{r}, \quad u^* = \left(\frac{\beta\hat{\Phi}_0}{V}\right)^2 \bar{u} \quad (21)$$

where

$$\bar{r} = \frac{N(x^*) - 1}{N(x^*) - s^{-2}}\bar{q}, \quad \bar{u} = \frac{3}{(x^*)^2}\left(\frac{1 - s^{-2}}{N(x^*) - s^{-2}}\right)^2 \bar{q}^2.$$

We consider potentials with $\hat{\Phi}_0 < 0$. Thus, we write $\hat{\Phi}_0 = -|\hat{\Phi}_0|$

Let us use the linear approximation for the recurrence relations (20)

$$\begin{pmatrix} r_{n+1} - r^* \\ u_{n+1} - u^* \end{pmatrix} = \mathcal{R} \begin{pmatrix} r_n - r^* \\ u_n - u^* \end{pmatrix}. \tag{22}$$

The elements of the linearized renormalization group transformation matrix $\mathcal{R}$ are calculated by the formulas

$$R_{11} = \left(\frac{\partial r_{n+1}}{\partial r_n}\right)^* = s^2 \left[N(x^*) + x^* \left(\frac{\partial N(x)}{\partial x}\right)_{x=x^*}\right],$$

$$R_{12} = \left(\frac{\partial r_{n+1}}{\partial u_n}\right)^* = \frac{R_{12}^{(0)}}{\sqrt{u^*}},$$

$$R_{21} = \left(\frac{\partial u_{n+1}}{\partial r_n}\right)^* = R_{21}^{(0)}\sqrt{u^*},$$

$$R_{22} = \left(\frac{\partial u_{n+1}}{\partial u_n}\right)^* = s\left[E(x^*) - \frac{x^*}{2}\left(\frac{\partial E(x)}{\partial x}\right)_{x=x^*}\right].$$

Here, the star refers to the fixed-point values, and

$$R_{12}^{(0)} = -\frac{s^2}{2\sqrt{3}}(x^*)^2 \left(\frac{\partial N(x)}{\partial x}\right)_{x=x^*},$$

$$R_{21}^{(0)} = s\sqrt{3}\left(\frac{\partial E(x)}{\partial x}\right)_{x=x^*}.$$

Note that the following relations were used for calculating the matrix elements:

$$\left(\frac{\partial x_n}{\partial r_n}\right)^* = \frac{\sqrt{3}}{\sqrt{u^*}}, \quad \left(\frac{\partial x_n}{\partial u_n}\right)^* = -\frac{x^*}{2u^*}.$$

The eigenvalues for the matrix $\mathcal{R}$ are

$$E_1 = \frac{1}{2}\Big\{(R_{11} + R_{22}) + \\ + \left[(R_{11} - R_{22})^2 + 4R_{12}^{(0)}R_{21}^{(0)}\right]^{1/2}\Big\},$$

$$E_2 = \frac{1}{2}\Big\{(R_{11} + R_{22}) - \\ - \left[(R_{11} - R_{22})^2 + 4R_{12}^{(0)}R_{21}^{(0)}\right]^{1/2}\Big\}.$$

The eigenvectors for the matrix $\mathcal{R}$ are

$$W_1 = W_{11}\begin{pmatrix} 1 \\ R_1 \end{pmatrix}, \quad W_1 = W_{11}\begin{pmatrix} R \\ 1 \end{pmatrix},$$

where constants W_{11} and W_{22} are to be determined, and quantities R and R_1 are defined as

$$R = \frac{R_{12}}{E_2 - R_{11}} = (u^*)^{1/2}R^{(0)},$$

$$R_1 = \frac{E_1 - R_{11}}{R_{12}} = (u^*)^{-1/2}R_1^{(0)}$$

with

$$R^{(0)} = \frac{R_{12}^{(0)}}{E_2 - R_{11}},$$

$$R_1^{(0)} = \frac{E_1 - R_{11}}{R_{12}^{(0)}}.$$

Thus, the solution to the linear recurrence relations (22) can be written as

$$\begin{pmatrix} r_n - r^* \\ u_n - u^* \end{pmatrix} = c_1' W_1 E_1^n + c_2' W_2 E_2^n, \tag{23}$$

where c_1' and c_2' are some constants. We arrive at the following equations for r_n and u_n:

$$\begin{aligned} r_n &= r^* + c_1 E_1^n + c_2 R E_2^n, \\ u_n &= u^* + c_1 R_1 E_1^n + c_2 E_2^n, \end{aligned} \tag{24}$$

where $c_1 = W_{11}c_1'$ and $c_2 = W_{22}c_2'$ are to be determined from the initial conditions at $n = 0$:

$$r_0 = a_2 + \frac{\beta\hat{\Phi}_0}{V}, \quad u_0 = a_4,$$

that leads to

$$\begin{aligned} c_1 &= (r_0 - r^* - (u_0 - u^*)\,R)D^{-1}, \\ c_2 &= (u_0 - u^* - (r_0 - r^*)\,R_1)D^{-1}, \end{aligned}$$

where

$$D = 1 - R_1 R = \frac{E_1 - E_2}{R_{11} - E_2}.$$

Numerical values of coefficients we have defined so far are presented in Table 1.

Table 1. **Numerical values for universal coefficients calculated at $x^* = 0$. These are independent of either the interaction potential or the potential averaging details during the layer-by-layer integration**

s^*	R_{11}	R_{22}	$R_{12}^{(0)}$	$R_{21}^{(0)}$
3.5862	7.6315	1.0000	3.8502	1.1753
E_1	E_2	D	$R^{(0)}$	$R_1^{(0)}$
8.2552	0.3763	1.0860	–0.5307	0.1620

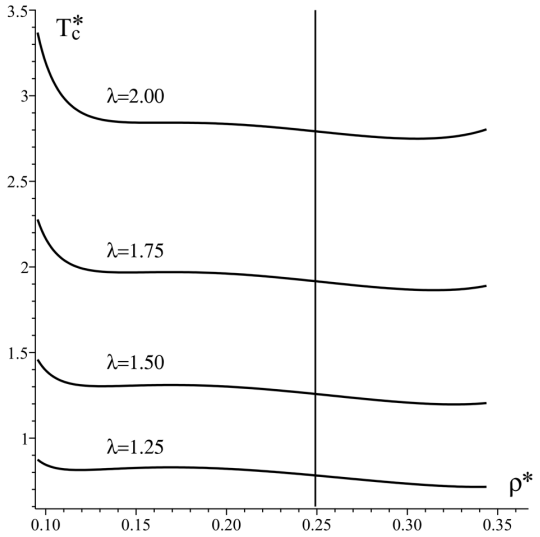

Critical temperature from Eq. (25) versus reduced density ρ^*. As an example, the square-well potential is used with different values of parameter λ (for details, see Section 4). The vertical line corresponds to the critical density $\rho_c^* = 0.249$ from [6]. Intersection of this line with a line $T_c^* = T_c^*(\rho^*)$ determines the critical temperature for particular potential

The fixed point solution should obey the recurrence relations at the critical point. Since $E_1 > 1$, it follows that the condition

$$c_1(T_c) = 0$$

must be true. In the explicit form, c_1 is written as

$$c_1 = \left[a_2 - (1 - \bar{r} - R^{(0)}\sqrt{\bar{u}})\frac{\beta|\hat{\Phi}_0|}{V} + \right.$$
$$\left. + \frac{a_4 R^{(0)}}{\sqrt{\bar{u}}}\left(\frac{\beta|\hat{\Phi}_0|}{V}\right)^{-1}\right] D^{-1},$$

and we arrive at the equation for the critical temperature

$$\left(1 - \bar{r} - R^{(0)}\sqrt{\bar{u}}\right)\left(\frac{\beta|\hat{\Phi}_0|}{V}\right)^2 -$$
$$- a_2\frac{\beta|\hat{\Phi}_0|}{V} + \frac{a_4 R^{(0)}}{\sqrt{\bar{u}}} = 0,$$

which is a quadratic equation for $\beta|\hat{\Phi}_0|/V$. From two solutions to this equation, we select the one that gives positive value for the critical temperature $T_c^* \equiv k_{\mathrm{B}}T_c/\varepsilon$:

$$T_c^* = \frac{|\hat{\Phi}_0|}{\varepsilon V}\frac{2(1 - \bar{r} - R^{(0)}\sqrt{\bar{u}})}{a_2 + \sqrt{a_2^2 - \frac{4a_4 R^{(0)}}{\sqrt{\bar{u}}}(1 - \bar{r} - R^{(0)}\sqrt{\bar{u}})}}. \quad (25)$$

We have obtained an explicit expression for the critical temperature in terms of the Fourier transform of the long-range part of the interaction potential in the long-wave limit, i.e., at $|\mathbf{k}| = 0$, of coefficients a_2 and a_4, which are calculated only based on the RS, and on the details of averaging the potentials along the layer-by-layer integration.

Note also that the value of the critical temperature depends on the density of the RS. One possible approach to find the critical value of ρ_c is from the condition that the average number of particles of the RS is equal to that of the whole system $\langle N\rangle_{\mathrm{RS}} = \langle N\rangle$, see [7] for details. This condition is essentially a mean field approximation for the critical density [16, 17], but since the dependence of T_c^* on ρ is smooth, see Figure, we will use the critical value of $\rho_c^* = 0.24912$ found from this condition in [6] (expressed there via critical value of the packing fraction $\eta_c = \frac{\pi}{6}\rho_c^* = 0.13044$).

In Section 4 we will calculate numerical values for T_c^* following from Eq. (25) for a few model systems of type "hard spheres with long-range attractive tail", and compare the results obtained from our analytic approach with known results from other works. For the HC system, we employ the Carnahan–Starling approximation [18] to calculate quantities a_2 and a_4, which enter the equation (25) and are explicitly given in Appendix A. But first let us discuss the details of interaction potentials and applied approximations for them.

3. Interaction Potentials. Parabolic Approximation

The potential energy of the inter-particle interaction is written in the form

$$U_N(\mathbf{r}^N) = \frac{1}{2}\sum_{\substack{i=1\\ i\neq j}}^{N}\sum_{j=1}^{N}\Psi(r_{ij}) + \frac{1}{2}\sum_{\substack{i=1\\ i\neq j}}^{N}\sum_{j=1}^{N}\Phi(r_{ij}).$$

Here $\Psi(r)$ corresponds for the short-range repulsive interaction, and $\Phi(r)$ for the long-range attractive interaction. In this work, the HC potential is taken for $\Psi(r)$

$$\Psi(r) = \begin{cases}\infty, & r \le \sigma,\\ 0, & r > \sigma,\end{cases}$$

where σ denotes the HC diameter. The long-range term $\Phi(r)$ is chosen so that it possesses a potential

well at $r \geq \sigma$

$$\Phi(r) = \begin{cases} 0, & r \leq \sigma, \\ \phi(r), & r > \sigma, \end{cases} \tag{26}$$

where $\phi(r)$ denotes the attractive part of the interaction and is chosen in the form of a few widely used potentials later. Separation in (26) is not the only way to select the form for $\Phi(r)$ inside the HC region. One popular approach is the Weeks–Chandler–Andersen (WCA) regularization originated from [19], according to which one has

$$\Phi(r) = \begin{cases} -\varepsilon, & r \leq r_{\mathrm{m}}, \\ \phi(r), & r > \sigma, \end{cases} \tag{27}$$

where r_{m} is the coordinate of the potential minimum. We use the WCA regularization scheme for most of the potentials considered in Section 4.

It is additionally assumed that the attractive part of the interaction potential possesses a well-behaved Fourier component $\hat{\Phi}_{\mathbf{k}}$ such that:

$$\Phi(r) = \frac{1}{V} \sum_{\mathbf{k}} \hat{\Phi}_{\mathbf{k}} \mathrm{e}^{i\mathbf{kr}} = \frac{1}{(2\pi)^3} \int \hat{\Phi}_{\mathbf{k}} \mathrm{e}^{i\mathbf{kr}} \mathrm{d}\mathbf{k},$$

and

$$\hat{\Phi}_{\mathbf{k}} = \int \Phi(r) \mathrm{e}^{-i\mathbf{kr}} \mathrm{d}\mathbf{r}.$$

Converting to spherical coordinates, and integrating over the angle variables, one arrives at

$$\hat{\Phi}(k) = \frac{4\pi}{k} \int_0^\infty r\Phi(r) \sin(kr)\, \mathrm{d}r. \tag{28}$$

Several model potentials will be considered for ϕ in the next Section 4.

To proceed with analytic calculations of the critical temperature and in order to get some numerical results, let us apply the so-called parabolic approximation for the Fourier component of the interaction potential

$$\hat{\Phi}_{\mathbf{k}} = \hat{\Phi}_0(1 - 2b^2k^2),$$

where

$$2b^2 = -\frac{1}{2\hat{\Phi}_0} \frac{\partial^2 \hat{\Phi}_k}{\partial k^2}\bigg|_{k=0}.$$

Then we select the cut-off parameter as

$$B_0 = \frac{1}{\sqrt{2}b}.$$

For $\hat{\Phi}_{B_{n+1},B_n}$, in the case of arithmetic average, it follows

$$\hat{\Phi}_{B_{n+1},B_n} = \hat{\Phi}_0 \left(1 - s^{-2n} \frac{1 + s^{-2}}{2}\right)$$

and for q one obtains

$$q = -\frac{\beta\hat{\Phi}_0}{V} \bar{q}, \quad \bar{q} = \frac{1 + s^{-2}}{2}$$

with $\bar{q} = 0.5389$.

In the case of spherical averaging

$$\hat{\Phi}_{B_{n+1},B_n} = \frac{\int_{B_{n+1}}^{B_n} \hat{\Phi}_{\mathbf{k}} \mathrm{d}\mathbf{k}}{\int_{B_{n+1}}^{B_n} \mathrm{d}\mathbf{k}} = \\ = \frac{\hat{\Phi}_0 \int_{B_{n+1}}^{B_n} (1 - 2b^2k^2)k^2 \mathrm{d}k}{\int_{B_{n+1}}^{B_n} k^2 \mathrm{d}k}, \tag{29}$$

one gets

$$\hat{\Phi}_{B_{n+1},B_n} = \hat{\Phi}_0 \left(1 - s^{-2n} \frac{3(1 - s^{-5})}{5(1 - s^{-3})}\right)$$

and, for q,

$$q = -\frac{\beta\hat{\Phi}_0}{V} \bar{q}, \quad \bar{q} = \frac{3(1 - s^{-5})}{5(1 - s^{-3})},$$

with $\bar{q} = 0.6123$ at $s = s^*$.

For convenience, we gathered the numerical values of coefficients depending on the potential averaging details in Table 2.

4. Results. Critical Temperature for Model Interaction Potentials

In this section we present numerical results for critical temperature calculated by Eq. (25) for several HC van der Waals models [20]. We consider the following potentials as the long-range attractive part of the whole interaction: the Morse potential, square-well potential, Yukawa potential, and Lennard-Jones

Table 2. **Numerical values for non-universal coefficients calculated at $x^* = 0$. These are dependent on the details of potential averaging during the layer-by-layer integration**

Averaging	$\bar{q}$	$\bar{r}$	$\bar{u}$
Arithmetic	0.5389	0.5389	0.6890
Spherical	0.6123	0.6123	0.8894

6-12 potential. For potential averaging, we apply the spherical one (29).

We start with the Morse potential given by

$$\phi^M(r) = \varepsilon\left\{\mathrm{e}^{-2(r-R_0)/\alpha} - 2\mathrm{e}^{-(r-R_0)/\alpha}\right\}.$$

This potential is characterized by the ratio of its parameters R_0/α. With increasing R_0/α, the range of interaction decreases, or, in other words, the potential well becomes narrower. Its Fourier transform is

$$\hat{\phi}^M_{\mathbf{k}} = -16\pi\varepsilon\alpha^3\mathrm{e}^{R_0/\alpha}\left[\frac{1}{(1+\alpha k^2)^2} - \frac{\mathrm{e}^{R_0/\alpha}}{(4+\alpha^2k^2)^2}\right],$$

and the Fourier transform $\hat{\Phi}_{\mathbf{k}}$ is

$$\hat{\Phi}_k = -16\pi\varepsilon\alpha^3 \times$$

$$\times\left[\frac{1}{1+k^2\alpha^2}\left(\frac{\sigma}{\alpha}+\frac{2}{1+k^2\alpha^2}\right)\cos(k\sigma) - \right.$$
$$-\frac{1}{4+k^2\alpha^2}\left(\frac{\sigma}{\alpha}+\frac{4}{4+k^2\alpha^2}\right)\cos(k\sigma)+$$
$$+\frac{\sigma/\alpha}{1+k^2\alpha^2}\left(\frac{\sigma}{\alpha}+\frac{1-k^2\alpha^2}{1+k^2\alpha^2}\right)\frac{\sin(k\sigma)}{k\sigma} -$$
$$\left.-\frac{\sigma/\alpha}{4+k^2\alpha^2}\left(2\frac{\sigma}{\alpha}+\frac{4-k^2\alpha^2}{4+k^2\alpha^2}\right)\frac{\sin(k\sigma)}{k\sigma}\right].$$

Table 3. **Critical temperature for different values of R_0/α**

HC Morse	
R_0/α	T_c^*
2.0	4.2852
2.5	2.1593
3.0	1.3418
3.5	0.9396
4.0	0.7096
4.5	0.5641
5.0	0.4652

Table 4. **Critical temperature of the HC square-well fluid for different values of λ**

Square-well		
λ	T_c^* (WCA)	T_c^* [20]
1.25	0.78	0.75
1.50	1.26	1.25
1.75	1.92	1.88
2.00	2.79	2.72

The results for critical temperature for the HC Morse model are presented in Table 3. It is seen from the results that the critical temperature decreases, as the range of interaction decreases. This trend is a common fact [20,21]. We have not found other works that study the HC Morse fluid, but we include these results here, since it has been the model often considered in the CV approach with HC as a RS [2, 6, 22], as well as without employing any RS [23, 24].

We proceed with the square-well potential given by

$$\phi^{SW}(r) = \begin{cases}\infty, & r \le \sigma,\\ -\varepsilon, & \sigma < r \le \lambda\sigma,\\ 0, & r > \sigma.\end{cases}$$

This potential is characterized by the parameter λ. Increasing λ one increases the width of the square well, and, thus, the range of interaction increases. Its Fourier transform does not exist, and the Fourier transform $\hat{\Phi}_{\mathbf{k}}$ in this case is

$$\hat{\Phi}_k = -\frac{4\pi\varepsilon\sigma^3}{(\sigma k)^3}\left[\sin(\lambda\sigma k) - \lambda\sigma k\cos(\lambda\sigma k) - \right.$$
$$\left.-\sin(\sigma k) + \sigma k\cos(\sigma k)\right].$$

We, however, will apply the WCA regularization for the square-well potential in the HC region

$$\Phi(r) = \begin{cases}-\varepsilon, & r \le \sigma,\\ \phi^{SW}(r), & r > \sigma,\end{cases}$$

since for such choice the agreement of critical temperature values with known results for this model is much better. The Fourier transform $\hat{\Phi}_{\mathbf{k}}$ in this case is

$$\hat{\Phi}_k = -\frac{4\pi\varepsilon\sigma^3}{(\sigma k)^3}\left[\sin(\lambda\sigma k) - \lambda\sigma k\cos(\lambda\sigma k)\right].$$

The results for such model are presented in Table 4. The results are compared with the ones reported in [20] for their perturbed virial expansion of the second order (PVE2). The work [20] contains more results for the HC square-well model obtained by different methods, as well as references to computer simulation results. As is seen from the results, the critical temperature increases as the range of interaction increases. Overall, the agreement of the

critical temperature for the square-well potential obtained within our approach agrees very well with the known results for this model.

The next one is the Yukawa potential given by

$$\phi^Y(r) = -\frac{\varepsilon\sigma}{r}\exp[-\lambda(r/\sigma - 1)]. \tag{30}$$

It is characterized by the parameter λ. With increasing λ the potential well gets narrower, thus, the range of interaction decreases. Its Fourier transform is

$$\hat{\phi}^Y_{\mathbf{k}} = -\frac{4\pi\varepsilon\sigma^3 \mathrm{e}^{\lambda}}{\lambda^2 + \sigma^2 k^2},$$

and the Fourier transform $\hat{\Phi}_{\mathbf{k}}$ is

$$\hat{\Phi}_k = -\frac{4\pi\varepsilon\sigma^3}{(\lambda^2 + \sigma^2 k^2)}\left[\cos(\sigma k) + \lambda\frac{\sin(\sigma k)}{\sigma k}\right].$$

Applying the WCA regularization, we get

$$\phi^Y(r) = \begin{cases} -\varepsilon, & r \le \sigma, \\ -\dfrac{\varepsilon\sigma}{r}\exp[-\lambda(r/\sigma - 1)], & r > \sigma, \end{cases} \tag{31}$$

and, thus,

$$\hat{\Phi}_k = -4\pi\varepsilon\sigma^3\left\{\frac{\sin(\sigma k) - \sigma k\cos(\sigma k)}{(\sigma k)^3} + \right.$$
$$\left. + \frac{1}{(\lambda^2 + \sigma^2 k^2)}\left[\cos(\sigma k) + \lambda\frac{\sin(\sigma k)}{\sigma k}\right]\right\}.$$

The results for the critical temperatures of the HC attractive Yukawa model (30) are presented in Table 5. They are compared with the ones reported in [21] (wherein other results for the critical temperature of the HC Yukawa model can also be found). As is seen from the Table 5, the critical temperature decreases, as the range of interaction decreases. Our results are reported for two cases, with and without applying the WCA regularization. It is seen that the critical temperature calculated without applying WCA regularization tends to be lower compared to the known results, while the one with applying it tends to be higher.

The final potential we consider in this paper is the Lennard-Jones one

$$\phi^{\mathrm{LJ}}(r) = 4\varepsilon\left[(\sigma/r)^{12} - (\sigma/r)^6\right].$$

The HC Lennard-Jones fluid is defined in literature [25, 26] as

$$\phi^{\mathrm{LJ}}(r) = \begin{cases} \infty, & r \le \sigma, \\ -\varepsilon, & \sigma < r \le r_{\mathrm{m}}, \\ 4\varepsilon\left[(\sigma/r)^{12} - (\sigma/r)^6\right], & r > r_{\mathrm{m}}, \end{cases}$$

Table 5. **Critical temperature of the HC Yukawa fluid for different values of λ**

HC Yukawa			
λ	T_c^*	T_c^* (WCA)	T_c^* [21]
0.5	6.15	7.24	7.009
1.0	2.07	2.69	2.486
1.5	1.16	1.69	1.634
1.8	0.90	1.41	1.228
2.0	0.79	1.28	1.031
2.5	0.59	1.07	0.836
3.0	0.47	0.94	0.722

Table 6. **Critical temperature of the HC Lennard-Jones fluid**

HC Lennard–Jones	
T_c^* (WCA)	T_c^* [25]
1.43	1.375

where $r_{\mathrm{m}} = 2^{1/6}\sigma$. In this case, it is easy to apply the WCA regularization

$$\Phi(r) = \begin{cases} -\varepsilon, & r \le r_{\mathrm{m}}, \\ 4\varepsilon\left[(\sigma/r)^{12} - (\sigma/r)^6\right], & r > r_{\mathrm{m}}. \end{cases} \tag{32}$$

We do not present the explicit formula for the Fourier transform of the potential defined by (32), since it is somewhat cumbersome, but its calculation by (28) is straightforward. The calculated critical temperature is present in Table 6. Result from [25] is given for comparison.

5. Conclusions

By integrating the functional for the grand partition function of a system of many interacting particles using the "layer-by-layer" approach, we have obtained a sequence of effective block Hamiltonians, each characterized by its own coefficients. Since the approach is essentially analytic and the coefficients are explicitly known, we derived the recurrence relations. The analysis of these recurrence relations revealed the existence of a fixed-point solution. We determined the coordinates of the fixed point and presented a solution linearized near the fixed point. By requiring that the linearized solution equals the fixed-point solution at large iteration numbers n, we derived an explicit

equation for the critical temperature T_c^* as a function of the particle density ρ^*. Using the critical density value from another work [6], we found the critical temperature that depends only on the parameters of the attractive part of the interaction potential. Based on this equation, we calculated the critical temperature for several hard-core van der Waals fluids and compared these values with known results for the considered models. The results confirm that the critical temperature of simple fluid models decreases, as the range of attractive interaction decreases.

R.V. Romanik acknowledges financial support from the National Research Foundation of Ukraine (Project No. 2023.03/0201) and is grateful to O.L. Ivankiv for comprehensive support, and to M.P. Kozlovskii for fruitful scientific discussions.

APPENDIX A.
Explicit Expressions for Quantities Entering the GPF Functional

Here, we explicitly present quantities entering the GPF expressions (2) and (3).

First, for the coefficients in (2) one has

$$\tilde{\mathfrak{M}}_0 = \langle N\rangle_0 \left[\tilde{\mathfrak{m}}_0 + \left(h + \frac{\mathfrak{m}_3}{\mathfrak{m}_4}\right)\tilde{\mathfrak{m}}_1 - \frac{\beta\hat{\Phi}_0}{2}\frac{\langle N\rangle_0}{V}\tilde{\mathfrak{m}}_1^2\right],$$

$$\tilde{\mathfrak{m}}_0 = -\frac{\mathfrak{m}_1\mathfrak{m}_3}{\mathfrak{m}_4} + \frac{\mathfrak{m}_2\mathfrak{m}_3^2}{2\mathfrak{m}_4^2} - \frac{\mathfrak{m}_3^4}{8\mathfrak{m}_4^2},$$

$$\tilde{\mathfrak{m}}_1 = \mathfrak{m}_1 - \frac{\mathfrak{m}_2\mathfrak{m}_3}{\mathfrak{m}_4} + \frac{\mathfrak{m}_3^3}{3\mathfrak{m}_4^2},$$

where $\langle N\rangle_0$ is the average particle number for the RS, and

$$\mathfrak{m}_1 = 1,$$
$$\mathfrak{m}_2 = 1 + \rho\hat{h}^{(2)},$$
$$\mathfrak{m}_3 = 1 + 3\rho\hat{h}^{(2)} + \rho^2\hat{h}^{(3)},$$
$$\mathfrak{m}_4 = 1 + 7\rho\hat{h}^{(2)} + 6\rho^2\hat{h}^{(3)} + \rho^3\hat{h}^{(4)}.$$

Here $\hat{h}^{(n)}$ are the Fourier transforms of the total correlation functions at $|\mathbf{k}| = 0$, and $\mathfrak{m}_n$ are the n-particle structure factors at $|\mathbf{k}| = 0$, both determined for the RS. They are functions of the RS particle density. More detailed investigation of quantities $\mathfrak{m}_n$ and $\hat{h}^{(n)}$ was performed in [7, 8].

The quantity h stands for

$$h = \beta(\mu - \mu_0),$$

where μ and μ_0 are the chemical potentials of the whole system and of the RS, respectively.

The quantity $Q(\tilde{\mathfrak{M}}_2, \mathfrak{M}_4)$ is determined by

$$Q(\tilde{\mathfrak{M}}_2, \mathfrak{M}_4) = \frac{1}{2\sqrt{\pi}}\left(\frac{12}{N_0\langle N\rangle_0|\mathfrak{m}_4|}\right)^{1/4} \mathrm{e}^{y^2/2}U(0,y),$$

where

$$y = \left(\frac{\langle N\rangle_0}{N_0}\frac{3\tilde{\mathfrak{m}}_2^2}{|\mathfrak{m}_4|}\right)^{1/2},$$

$$\tilde{\mathfrak{m}}_2 = \mathfrak{m}_2 - \frac{\mathfrak{m}_3^2}{2\mathfrak{m}_4},$$

and $U(a,y)$ is the Weber parabolic cylinder function [27].

Now, for quantities in (3) we have

$$a_2 = \left(\frac{3}{N_0\langle N\rangle_0|\mathfrak{m}_4|}\right)^{1/2} U(y),$$

$$a_4 = \frac{3}{N_0\langle N\rangle_0|\mathfrak{m}_4|}\varphi(y),$$

where

$$U(y) = \frac{U(1,y)}{U(0,y)},$$

$$\varphi(y) = 3U^2(y) + 2yU(y) - 2.$$

By multiplying a_2 by $\langle N\rangle_0$, and a_4 by $\langle N\rangle_0^2$, we get quantities that are functions of the particle density only

$$a_2^{'} = \langle N\rangle_0 a_2,$$
$$a_4^{'} = \langle N\rangle_0^2 a_4.$$

Finally, the quantity μ^* is a linear function of the chemical potential μ

$$\mu^* = h + \frac{\mathfrak{m}_3}{\mathfrak{m}_4} + \frac{\langle N\rangle_0}{V}\beta\hat{\Phi}_0\tilde{\mathfrak{m}}_1.$$

APPENDIX B. Some relations for site variables

Here, we present some relations between sets of CV $\{\rho_{\mathbf{k}}, \omega_{\mathbf{k}}\}$ and their counterparts – site CV $\{\tilde{\rho}_{\mathbf{l}}, \tilde{\omega}_{\mathbf{l}}\}$. The presented expressions are meant to be generic, so that the meaning of summation over $\mathbf{k}$ and over $\mathbf{l}$ are not particularly specified, while N being the number of different values that $\mathbf{k}$ or $\mathbf{l}$ takes on. They are usually specified more strictly in particular applications.

By definition

$$\tilde{\omega}_{\mathbf{l}} = \frac{1}{\sqrt{N}}\sum_{\mathbf{k}}\omega_{\mathbf{k}}\mathrm{e}^{-\mathrm{i}\mathbf{k}\mathbf{l}},$$

$$\tilde{\rho}_{\mathbf{l}} = \frac{1}{\sqrt{N}}\sum_{\mathbf{k}}\rho_{\mathbf{k}}\mathrm{e}^{\mathrm{i}\mathbf{k}\mathbf{l}}.$$

From this definition, the following equalities follow:

$$\sum_{\mathbf{l}}\tilde{\omega}_{\mathbf{l}}\tilde{\rho}_{\mathbf{l}} = \sum_{\mathbf{k}}\omega_{\mathbf{k}}\rho_{\mathbf{k}}.$$

$$\sum_{\mathbf{l}}\tilde{\omega}_{\mathbf{l}}^2 = \sum_{\mathbf{k}}\omega_{\mathbf{k}}\omega_{-\mathbf{k}},$$

$$N\sum_{\mathbf{l}}\tilde{\omega}_{\mathbf{l}}^4 = \sum_{\mathbf{k_1},\ldots,\mathbf{k_4}}\omega_{\mathbf{k}_1}\ldots\omega_{\mathbf{k}_4}\delta_{\mathbf{k}_1+\ldots+\mathbf{k}_4},$$

$$N^{\frac{n}{2}-1}\sum_{\mathbf{l}}\tilde{\omega}_{\mathbf{l}}^n = \sum_{\mathbf{k}_1,\ldots,\mathbf{k}_n}\omega_{\mathbf{k}_1}\ldots\omega_{\mathbf{k}_n}\delta_{bfk_1+\ldots+\mathbf{k}_n}.$$

$$\sum_{\mathbf{l}}\tilde{\rho}_{\mathbf{l}}^2 = \sum_{\mathbf{k}}\rho_{\mathbf{k}}\rho_{-\mathbf{k}},$$

$$N\sum_{\mathbf{l}}\tilde{\rho}_{\mathbf{l}}^4 = \sum_{\mathbf{k_1},\ldots,\mathbf{k_4}}\rho_{\mathbf{k}_1}\ldots\rho_{\mathbf{k}_4}\delta_{bfk_1+\ldots+\mathbf{k}_4},$$

$$N^{\frac{n}{2}-1}\sum_{\mathbf{l}}\tilde{\rho}_{\mathbf{l}}^n = \sum_{\mathbf{k}_1,\ldots,\mathbf{k}_n}\rho_{\mathbf{k}_1}\ldots\rho_{\mathbf{k}_n}\delta_{\mathbf{k}_1+\ldots+\mathbf{k}_n}.$$

1. I.R. Yukhnovskii, M.F. Holovko. *Statistical Theory of Classical Equilibrium Systems* (Naukova dumka, 1980) [in Russian].
2. I.R. Yukhnovskii. The functional of the grand partition function for the investigation of the liquid-gas critical point. *Physica A* **168**, 999 (1990).
3. I.R. Yukhnovskii. Phase transitions in a vicinity of the vapor-liquid critical point. *Ukr. J. Phys.* **10**, 33 (2015) [in Ukrainian].
4. J.P. Hansen, I.R. McDonald. *Theory of Simple Liquids: With Applications to Soft Matter* (Academic Press, 2013) [ISBN: 9780123870339].
5. I.I. Adamenko, L.A. Bulavin. *Physics of Liquids and Liquid Systems* (ASMI, 2006) [in Ukrainian] [ISBN: 966-7653-32-3].
6. I.R. Yukhnovskii, I.M. Idzyk, V.O. Kolomiets. Investigation of a homogeneous many-particle system in the vicinity of the critical point. *J. Stat. Phys.* **80**, 405 (1995).
7. I.R. Yukhnovskii, R.V. Romanik. Grand partition function functional for simple fluids. *J. Phys. Stud.* **28**, 2602-1 (2024).
8. I.R. Yukhnovskii, R.V. Romanik. *Grand Partition Function Functional for Simple Fluids* (Preprint ICMP-23-01E, 2023).
9. I.R. Yukhnovskii, M.P. Kozlovskii, I.V. Pylyuk. *Microscopic Theory of Phase Transitions in the Three-Dimensional Systems* (Eurosvit, 2001) [in Ukrainian] [ISBN: 966-7343-26-X].
10. M.P. Kozlovskii. *Influence of an External Field on the Critical Behavior of Three-Dimensional Systems* (Halytskyi drukar, 2012) [in Ukrainian] [ISBN: 978-966-970-442-7].
11. M.P. Kozlovskii, R.V. Romanik. Influence of an external field on the critical behavior of the 3D Ising-like model. *J. Mol. Liq.* **167**, 14 (2012).
12. V.L. Kulinskii. Simple geometrical interpretation of the linear character for the zeno-line and the rectilinear diameter. *J. Phys. Chem. B* **114**, 2852 (2010).
13. L.A. Bulavin, V.L. Kulinskii. Generalized principle of corresponding states and the scale invariant mean-field approach. *J. Chem. Phys.* **133**, 134101 (2010).
14. I.R. Yukhnovskii. Solution of the three-dimensional Ising model for description of the second-order phase transition. *Riv. Nuovo Cimento* **12**, 1 (1989).
15. M.P. Kozlovskii. Recurrence relations for the three-dimensional Ising-like model in the external field. *Condens. Matter Phys.* **8**, 473 (2005).
16. J.-M. Caillol, O.V. Patsahan, I.M. Mryglod. The collective variables representation of simple fluids from the point of view of statistical field theory. *Condens. Matter Phys.* **8**, 665 (2005).
17. J.-M. Caillol, O.V. Patsahan, I.M. Mryglod. Statistical field theory for simple fluids: The collective variables representation. *Physica A* **368**, 326 (2006).
18. N.F. Carnahan, K.E. Starling. Equation of state for nonattracting rigid spheres. *J. Chem. Phys.* **51**, 635 (1969).
19. J.D. Weeks, D. Chandler, H.C. Andersen. Role of repulsive forces in determining the equilibrium structure of simple liquids. *J. Chem. Phys.* **54**, 5237 (1971).
20. J. Krejci, I. Nezbeda. The critical temperature and properties of real gas from low order perturbed virial expansions. *Fluid Phase Equilib.* **314**, 156 (2012).
21. E.B. El Mendoub, J.-F. Wax, N. Jakse. Evolution of the liquid-vapor coexistence of the hard-core Yukawa fluid as a function of the interaction range. *J. Chem. Phys.* **132**, 164503 (2010).
22. I.R. Yukhnovskii, O.V. Patsahan. Grand canonical distribution for multicomponent system in the collective variables method. *J. Stat. Phys.* **81**, 647 (1995).
23. I.V. Pylyuk, M.P. Kozlovskii, O.A. Dobush. Analytic calculation of the critical temperature and estimation of the critical region size for a fluid model. *Ukr. J. Phys.* **68**, 601 (2023).
24. I.V. Pylyuk, M.P. Kozlovskii, O.A. Dobush, M.V. Dufanets. Morse fluids in the immediate vicinity of the critical point: calculation of thermodynamic coefficients. *J. Mol. Liq.* **385**, 122322 (2023).
25. G.M. Sowers, S.I. Sandler. Equations of state from generalized perturbation theory. Part 1. The hard-core Lennard-Jones fluid. *Fluid Phase Equilib.* **63**, 1 (1991).
26. A. Diez, J. Largo, J.R. Solana. Excess energy and equation of state of fluids with hard-core potential models from a second-order Monte Carlo perturbation theory. *Fluid Phase Equilib.* **298**, 262 (2010).
27. F.W. Olver, D.W. Lozier, R. Boisvert, C.W. Clark. *The NIST Handbook of Mathematical Functions* (Cambridge University, 2010) [ISBN: 978-0521140638].

Received 12.07.24

І.Р. Юхновський, Р.В. Романік

ВИЗНАЧЕННЯ КРИТИЧНОЇ ТЕМПЕРАТУРИ ПРОСТИХ ПЛИНІВ: АНАЛІТИЧНИЙ ПІДХІД НА ОСНОВІ МЕТОДУ КОЛЕКТИВНИХ ЗМІННИХ

В рамках аналітичного підходу – методу колективних змінних із системою відліку – отримано явне рівняння для критичної температури рідина–пара простих плинів. Це рівняння застосовано для розрахунку значень критичної температури кількох твердосферних плинів Ван-дер-Ваальса. Також було досліджено, як критична температура залежить від параметрів взаємодії. Зокрема, виявлено, що зі зменшенням області притягальної взаємодії критична температура також зменшується.

Ключові слова: прості плини, колективні змінні, критична температура.